Redox Biology 37 (2020) 101758

Contents lists available at ScienceDirect

Redox Biology

journal homepage: www.elsevier.com/locate/redox

Research Paper

Protein thiol oxidation in the rat lung following e-cigarette exposure

Juan Wang [a,1], Tong Zhang [a,1], Carl J. Johnston [b], So-Young Kim [b], Matthew J. Gaffrey [a], David Chalupa [c], Guanqiao Feng [d], Wei-Jun Qian [a,***], Matthew D. McGraw [b,c,**], Charles Ansong [a,*]

[a] Biological Sciences Division, Pacific Northwest National Laboratory, Richland, WA, 99352, United States
[b] Department of Pediatric Pulmonology, University of Rochester Medical Center, Rochester, NY, 14642, United States
[c] Department of Environmental Medicine, University of Rochester Medical Center, Rochester, NY, 14642, United States
[d] Department of Biological Sciences, Texas Tech University, Lubbock, TX, 79409, United States

ARTICLE INFO

Keywords:
Electronic cigarette aerosol
Rat
Lung
Oxidative stress
Redox proteomics
Ubiquitin proteasome response (UPS)

ABSTRACT

E-cigarette (e-cig) aerosols are complex mixtures of various chemicals including humectants (propylene glycol (PG) and vegetable glycerin (VG)), nicotine, and various flavoring additives. Emerging research is beginning to challenge the "relatively safe" perception of e-cigarettes. Recent studies suggest e-cig aerosols provoke oxidative stress; however, details of the underlying molecular mechanisms remain unclear. Here we used a redox proteomics assay of thiol total oxidation to identify signatures of site-specific protein thiol modifications in Sprague-Dawley rat lungs following *in vivo* e-cig aerosol exposures. Histologic evaluation of rat lungs exposed acutely to e-cig aerosols revealed mild perturbations in lung structure. Bronchoalveolar lavage (BAL) fluid analysis demonstrated no significant change in cell count or differential. Conversely, total lung glutathione decreased significantly in rats exposed to e-cig aerosol compared to air controls. Redox proteomics quantified the levels of total oxidation for 6682 cysteine sites representing 2865 proteins. Protein thiol oxidation and alterations by e-cig exposure induced perturbations of protein quality control, inflammatory responses and redox homeostasis. Perturbations of protein quality control were confirmed with semi-quantification of total lung polyubiquitination and 20S proteasome activity. Our study highlights the importance of redox control in the pulmonary response to e-cig exposure and the utility of thiol-based redox proteomics as a tool for elucidating the molecular mechanisms underlying this response.

1. Introduction

Electronic cigarettes (e-cigs) are advertised as assistive devices for smoking cessation and a healthy substitute to tobacco with minimal-to-no harm. However, there is significant uncertainty as to the claimed a healthy outcome for users [1–4]. E-cig aerosol is a complex mixture of e-liquid components including but not limited to propylene glycol (PG), vegetable glycerin (VG), nicotine, water, and flavoring additives. Several studies have assessed the *in vivo* toxicity of different mixtures of individual e-liquid components [5–9]. Werley et al. assessed 7-day and 28-day inhalation toxicity of 100% PG in Sprague-Dawley rats and observed relatively low toxicity with mild nasal irritation and laryngeal squamous metaplasia [5]. Lechasseur et al. exposed BALB/c mice to 100% VG over an 8-week period and observed effects on the expression of circadian molecular clock genes in the exposed-lungs [7]. This study also provided transcriptomic data but with no apparent sign of lung inflammation. In a more comprehensive analysis, Phillips et al. exposed Sprague-Dawley rats to varying PG/VG mixtures with or without nicotine over a 90-day exposure regime (sub-chronic inhalation) [8]. Standard toxicological endpoints in the lung and liver complemented by molecular analyses using transcriptomics, proteomics, and lipidomics showed no signs of toxicity with limited molecular impacts.

While the aforementioned studies reported e-cigs having mild or no adverse effect on lung tissue in animal models as observed by

* Corresponding author.
** Corresponding author. Department of Pediatric Pulmonology, University of Rochester Medical Center, Rochester, NY, 14642, United States.
*** Corresponding author.
E-mail addresses: Weijun.Qian@pnnl.gov (W.-J. Qian), matthew_mcgraw@URMC.Rochester.edu (M.D. McGraw), cansong07@gmail.com (C. Ansong).
[1] Equal contributors.

https://doi.org/10.1016/j.redox.2020.101758
Received 17 July 2020; Received in revised form 21 August 2020; Accepted 8 October 2020
Available online 10 October 2020

histopathological and -omics analyses, other studies have detected redox imbalance and increased inflammatory response in lung tissue of animal models elicited by e-cig exposures [10–12]. Lerner et al. reported increased expression of pro-inflammatory cytokines and diminished lung glutathione (GSH) levels following acute (3-day) e-cig exposure in C57BL/6J mice [11]. Cirillo et al. exposed Sprague Dawley rats to e-cig aerosol for 28 days and assessed pulmonary inflammation, oxidative stress and tissue damage [10]. Tissue morphometric analysis demonstrated alterations in lung structure with large areas of airflow collapse and tissue disruption. Modulation of antioxidant and phase II enzymes suggested a perturbation of the lung redox status. Glynos et al. reported negligible changes in proinflammatory cytokines and lung histology following acute (3 days) and subchronic (4 weeks) exposure of mice to e-cig aerosols [12]. Further, three-day acute exposure, but not the 4-week subchronic exposure, significantly increased oxidative stress in lung tissue. Taken together, the prior studies described above support the notion that e-cig aerosol/vapor exposure induces oxidative stress and an inflammatory response in the lungs. However, details of the underlying molecular mechanisms remain unclear. Post-translational modifications (PTMs) of protein thiols in response to ROS/RNS provide important insights into the widespread consequences of inflammation and oxidative stress. Here we used a redox proteomics assay of thiol total oxidation to identify signatures of site-specific protein thiol modifications induced by e-cig exposures to provide new insights into e-cigarette-associated redox signaling in the lung.

2. Materials and methods

2.1. Animals

The studies were approved by the Institutional Animal Care and Use Committee of the University of Rochester Medical Center (URMC). The investigators adhered to the National Institutes of Health Guide for the Care and Use of Laboratory Animals (1996), and the research was carried out in compliance with the Animal Welfare Act.

Seven-week-old outbred male Charles River Sprague Dawley (SD) rats weighing 250 g–300 g (Charles River Laboratory, Wilmington, MA) were used in this study, maintained in an AAALAC-accredited animal care facility. All animals were provided commercially certified rat chow and water ad libitum. Rats were quarantined for 7 days following arrival to allow for acclimatization, housed two to three animals per cage, and their health status was monitored daily.

2.2. Chemicals & e-cigarette liquid

Propylene glycol (PG), vegetable glycerin (VG), and (−)-nicotine free base (>99% GC) were purchased from Sigma-Aldrich (St. Louis, MO). E-liquid consisting of 50% PG, 50% VG and, in certain conditions, 25 mg/mL nicotine was prepared on the day of exposure.

2.3. Aerosol generation and characterization

E-cigarette aerosol was generated using the InExpose tank system extension (E-cig mod; SciReq, Montreal, CA). The puff profile used for the exposure included a total volume of 70 mL, an exposure time of 3.3 s, with a sinusoidal wave, every 30 s (2 puffs per minute) with a bias flow of 2 L/min between puffs for 60 min. The e-cigarette atomizer consisted of a nickel-based, temperature-controlled coil with 0.15 Ohm resistance with stainless steel housing and cotton-based wick (sub-ohm coil, KangerTech, Shenzhen, China). The aerosol generated was characterized for total particulate mass (TPM), mass median aerodynamic diameter (MMAD), and geometric standard deviation (GSD). Sampling from TPM, MMAD, and GSD was obtained from a nose-only port at a continuous flow of 250 mL/min for 10 min. A 25 mm Pallflex Emfab filter (Pall Corporation, Port Washington, NY) was weighed before and after sampling for TPM. MMAD and GSD were determined using a seven-stage cascade impactor (In-Tox Products, Moriarty, NM).

2.4. Animal exposures

Prior to exposure, 1 mL of e-cig liquid was dispensed onto the atomizer ensuring saturation of the cotton wick and prevention of a dry burn. Rats were exposed to e-cigarette aerosol for 3 h per day for 3 consecutive days via a nose-only exposure system (IET 200B Chambers, IES 324 Inhalation Tower; Electro-Medical Measurement System (EMMS), Bordon, Hampshire, UK). After 60 min of exposure, animals were rested for 30 min prior to the next exposure (total of 3 h of exposure per day). Control animals were housed in identical nose-only chambers and were exposed to humidified (30–50%) filtered air only.

2.5. Euthanasia

Animals were euthanized immediately following the last day of e-cigarette exposure. Euthanasia was performed via terminal sodium pentobarbital intraperitoneal (IP) injection (100 mg/kg; Abbott Laboratories, Abbott Park, IL) followed by diaphragmatic puncture and exsanguination.

2.6. Bronchoalveolar lavage fluid (BALF), tissue harvest and histopathology

After terminal anesthesia and exsanguination, lung tissue was cleared of blood by flushing the right ventricle with 10 mL phosphate-buffered solution (PBS). The trachea was then cannulated, left bronchus clamped, and the right lung was lavaged with two 2.5 mL washes of normal saline (0.9%) solution. Right lung lobes were tied off and immediately snap frozen (−80 °C) following 10 mL PBS flush. The left lung was then unclamped and intratracheally fixed with 10% neutral buffered formalin at 20 cm H_2O for 30 min prior to removal by gross dissection. Paraffin embedded tissues were sectioned at a thickness of 5 mm and stained for hematoxylin and eosin (H&E). BALF samples were pooled, centrifuged at 2000 g for 10 min at 4 °C, and supernatants frozen (−80 °C). Cell pellets from BALF were re-suspended using 1 mL PBS and cytospin slides (Thermo Shandon, Pittsburgh, PA) were prepared using 50,000 cells per slide. Differential cell counts (~400 cells/slide) were performed on cytospin-prepared slides stained with Diff-Quik (Siemens, DE). Total cell counts were expressed per microliter of BALF.

2.7. Cotinine assay

Cotinine levels were measured in rat serum collected immediately after the third day of e-cigarette aerosol exposure by ELISA according to the manufacturer's instructions (Abnova, Taipei, TW). Briefly, three ml of fresh blood was collected from the descending aorta prior to exsanguination. The blood was allowed to clot, centrifuged at 10,000 g for 20 min at 4 °C, and the serum was collected for further analysis. Absorbance was measured at 450 nm using a SpectraMax M5 plate reader (Molecular Devices, San Jose, CA). Samples with cotinine concentrations greater than 100 ng/mL required a 1:2 dilution.

2.8. Total glutathione (GSH) assay

Total glutathione (GSH) levels were measured by ELISA according to the manufacturer's instructions (Cayman Chemical, Ann Arbor, Michigan, USA). All samples used for GSH measurement underwent deproteination in metaphophoric acid (MPA) reagent prior to performing the assay. Total lung glutathione (GSH), both oxidized and reduced forms, was determined from the assay; quantification of GSSG alone, the oxidized form of GSH and exclusive of total GSH, required further derivation with 2-vinylpyridine, which was not performed. Considering the sulfhydryl group of GSH reacts with 5, 5′-dithio-bis-2-(nitrobenzoic acid) (DTNB) producing 5-thio-2-nitrobenzoic acid (TNB), the

concentration of total glutathione in the supernatant of lung homogenates was determined by measuring the absorbance of TNB at 405 nm. Results were expressed as the nmol of total glutathione (GSH) per mg total lung protein. All samples homogenates were prepared using RIPA buffer and underwent a single freeze thaw cycle prior to measuring glutathione levels.

2.9. Sample preparation for redox proteomics

The thiol-based redox proteomics experiments were performed as previously described [13–17]. Briefly, frozen rat lung tissues were minced on dry ice quickly into small pieces. To quantify total thiol, a small portion of tissues from the control and e-cig samples (n = 4 for each) were pooled and incubated in homogenization buffer consisting of 250 mM MES, pH 6.0, 1% sodium dodecyl sulfate (SDS), and 1% Triton-X-100. Aliquots of the original 8 tissue samples were incubated in homogenization buffer with 100 mM N-ethyl-maleimide (NEM). Following incubation for 30 min on ice in the dark, all samples were then homogenized using a hand-held homogenizer. The resulting homogenate was transferred to a 2.0 mL centrifuge tube and then centrifuged at 14,000 rpm at 4 °C for 10 min to remove insoluble material. Alkylation reaction was carried out at 55 °C and 850 rpm in dark for 30 min, followed by protein precipitation with cold acetone (−20 °C) over night. Protein pellets were resuspended in 250 mM 2-[4-(2-hydroxyethyl) piperazin-1-yl]ethanesulfonic acid (HEPES), pH 7.0, 8 M urea and 0.1% SDS. Protein concentration was determined using the bicinchoninic acid assay (BCA). For each sample, 500 μg of proteins were subjected to buffer exchange via a 0.5 mL 10 K Amicon ultra filter with 8 M urea in 25 mM HEPES, pH 7.0. Samples were diluted to 500 μL using 25 mM HEPES buffer with 1 M urea in 25 mM HEPES, pH 7.6 and then reduced with 20 mM Dithiothreitol (DTT) in the presence of 0.2% SDS at 37 °C for 30 min. Excess DTT was removed by buffer exchange, and BCA was performed to determine the protein concentration prior to thiol enrichment. For each sample, 150 μg of proteins were incubated with 30 mg of thiopropyl Sepharose 6B resin in of 25 mM HEPES, pH 7.6 with 0.2% SDS at room temperature for 2 h, 850 rpm. The resin was washed sequentially with 1) 8 M urea, 2) 2 M NaCl, 3) 80% acetonitrile (ACN) with 0.1% trifluoroacetic acid (TFA), and 4) 25 mM HEPES, pH 7.0, each buffer 5 times. On-resin protein digestion, TMT labeling, and elution of peptides from the resin were essentially carried out as previously described [14,15]. All samples were combined, desalted by solid phase extraction and store in −80 °C before LC-MS/MS analysis.

2.10. Liquid chromatography-tandem mass spectrometry (LC-MS/MS) analysis

Dried peptides were resuspended in H_2O and diluted to 0.1 μg/μL. An aliquot of 5 μL was injected to a Waters nanoACQUITY UPLC system coupled with Q Exactive plus mass spectrometer (Thermo Fisher Scientific). Peptide separation was performed with an in-house packed C18 column (50 cm × 75 μm i.d., Phenomenex Jupiter, 3 μm particle size) using a binary mobile system (buffer A: 0.1% formic acid in H_2O; buffer B: 0.1% formic acid in acetonitrile) with buffer B percentage increased linearly at the following points: 0.1% at 0 min, 8% at 4 min, 12% at 36 min, 30% at 135 min, 45% at 175 min, and 95% at 180 min.

A data-dependent acquisition method was used to collect mass spectra. Each cycle consisted of a full MS scan and up to 12 MS/MS scans of the most abundant precursor ions. Full MS scan was performed in the Orbitrap mass analyzer at 400–2000 *m/z* with the following key parameters: resolution 70,000; automatic gain control (AGC): 1e6, and maximum injection time (IT): 20 ms. For MS/MS, precursor ions were selected by the quadrupole mass analyzer at an isolation window of 2 *m/z*, and then fragmented by higher-energy collisional dissociation (HCD) of normalized collision energy at 30. The resulting MS/MS spectra were analyzed in the Orbitrap with the following settings: resolution: 35,500; scan range 200–2000 *m/z* with the fixed first mass of 110 *m/z*; AGC: 1e5; and maximum IT of 100 ms. A 30 s dynamic exclusion was also applied.

2.11. Western blot for Lys48-linked ubiquitin and ubiquitin-C

Rat lungs were homogenized in Radioimmunoprecipitation assay buffer (RIPA lysis buffer) (Abcam; Cambridge, MA) supplemented with a protease inhibitor cocktail (Roche; Indianapolis, IN). Following centrifugation at 12,000 rpm for 20 min at 4 °C, soluble supernatant fractions were collected for total protein and Western blot analysis. Total protein concentrations were determined by BCA assay kit (Thermo Scientific, Waltham, MA). 10 μg total protein were resolved in pre-casted 4–15% gradient Tris-Glycine 'Stain-Free' Mini-Protean gel (Bio-Rad, Hercules, CA) to assess for lysine (K)48-linked ubiquitin (1:1000, R&D Systems) and ubiquitin-C (1:1000, Invitrogen) expression. Gels were transferred to 0.1 μm nitrocellulose membrane (GE Healthcare). Horseradish peroxidase (HRP) and SuperSignal West Pico chemiluminescent substrates (Thermo Scientific) were used to detect protein signal intensity. Semi-quantification was performed using Image Lab software (Bio-Rad, Hercules, CA) and normalized relative to total protein imaged from the 'Stain-Free' gel.

2.12. 20S proteasome activity for rat lung homogenate

Rat lung was lysed and collected in 50 mM HEPES (pH 7.5), 5 mM Ethylenediaminetetraacetic acid (EDTA), 150 mM NaCl and 1% Triton X-100 supplemented with 2 mM ATP buffered solution. 20S proteasome activity was determined using the Chemicon 20S Proteasome Activity Assay (Millipore) according to the manufacturer's instructions. Luminescent signal was semi-quantified using a SpectraMax M5 plate reader (Molecular Devices, San Jose, CA). Enzymatic activity in e-cig-exposed samples was expressed as absolute activity (micrograms/milligram total rat lung) as well as relative activity to air controls.

2.13. Data analysis and statistics

Raw MS data was searched using MS-GF + against an Uniprot *Rattus norvegicus* protein database (31,823 entries, downloaded October 2017) [18]. Key search parameters were 20 ppm tolerance for precursor ion masses, 0.5 Da tolerance for fragment ions, dynamic oxidation of methionine (15.9949 Da), dynamic NEM modification of cysteine (125.0477 Da), and static 10-plex TMTs modification of lysine and peptide N-termini (229.1629 Da). The obtained peptide spectrum matches (PSMs) were filtered by 1) mass error within 10 ppm; and 2) PepQ value < 0.01, which controlled the false discovery rate (FDR) level below 1%. For quantitative analysis, MASIC was used to extract the reporter ion intensities from the raw data [19]. An in-house R script was used to link the peptide identifications and quantifications as described before [20]. Reporter ion intensities for PSMs corresponding to the same unique peptide were summed and log2 transformed. Peptides quantified in all samples were kept for further analysis.

The site occupancy of total oxidation was calculated as the ratio of the average level of total oxidation (n = 4 e-cig or control samples) over total thiol (n = 1 for the pooled sample) in percentage. Student t-test was used to determine the statistical significance between the control and E-cig groups. Significant cysteine-containing peptides were defined as 1) $p < 0.01$ and 2) at least 20% in fold change (ie, log2FC < −0.26 or log2FC > 0.26). Gene ontology analysis of significant proteins were performed with DAVID (https://david.ncifcrf.gov/summary.jsp). Functional and protein interaction network analysis was performed using Ingenuity pathway analysis (www.ingenuity.com).

3. Results

3.1. Aerosol characterization

E-cig aerosols were characterized for total particulate mass (TPM),

mass median aerodynamic diameter (MMAD), and geometric standard deviation (GSD). The average TPM for exposures was 0.968 ± 0.194 mg/mL. The average MMAD was 0.92 ± 0.04 μm, and the range GSD for all exposures was 1.4–1.6. This average TPM is similar to a medium concentration PG/VG exposure used for chronic studies in a prior rat e-cigarette exposure model [8].

3.2. E-cigarette exposures

Seven-week-old Sprague-Dawley rats (average weight: 254.0 ± 10.2 g) were exposed to humidified room air (n = 15), 50% propylene glycol: 50% vegetable glycerin (PG/VG) (n = 14), or PG/VG + 25 (2.5%) mg/mL nicotine (n = 17) for 3 h per day for 3 consecutive days via nose-only exposure. At the end of exposures, rat serum was collected for cotinine levels. Both air controls and PG/VG + 0% nicotine rats had plasma cotinine levels less than 5 ng/mL (0.0 ± 0.0 ng/mL and 0.7 ± 1.2 ng/mL, respectively). Serum cotinine levels increased significantly in PG/VG + 2.5% nicotine as shown in Fig. 1A (103.3 ± 10.5 ng/mL; ANOVA, ****p < 0.0001). Serum cotinine concentrations following acute exposure were similar in magnitude to that seen in newborn mice exposed to 1.8% nicotine with PG for ten days [21].

3.3. Histology and BALF analysis

Left lungs of all exposed rats were fixed, embedded and sectioned for further histologic evaluation following e-cigarette exposure. H&E stained lung sections from animals exposed to air, PG/VG + 0% nicotine and PG/VG + 2.5% nicotine displayed preserved lung structure of the distal lung parenchyma and intrapulmonary bronchioles with rare foci of inflammatory infiltrates in the alveolar cell walls (Fig. 1B). Consistent with histology, BAL total cell counts (Fig. 1C) did not differ significantly between air controls (503 ± 66 cell/μL), PG/VG (454 ± 65 cell/μL), and PG/VG + 2.5% nicotine (481 ± 137 cell/μL) (ANOVA, p = 0.57). BAL cell differential (Fig. 1C) also did not differ significant between groups with the average macrophage percent in air controls 92 ± 4%, PG/VG 91 ± 5%, and PG/VG + 2.5% nicotine 91 ± 4% (ANOVA, p = 0.77).

3.4. Decrease in total lung GSH

GSH was assessed immediately following the end of e-cigarette exposures as a surrogate marker of oxidative stress. Normalized GSH was significantly reduced in rat lungs exposed to PG/VG (1.41 ± 0.52 nM/mg and PG/VG + 2.5% nicotine (1.63 ± 1.12 nM/mg) compared to lungs exposed to air control (5.28 ± 0.95 nM/mg; ANOVA, ****p < 0.0001) as shown in Fig. 2. Normalized GSH did not differ between PG/VG and PG/VG + 2.5% nicotine exposed lungs (p = 0.78, ANOVA with Tukey's). Hence, acute e-cigarette exposure resulted in significant lung oxidative stress as demonstrated by reduced total lung glutathione and independent of nicotine concentration.

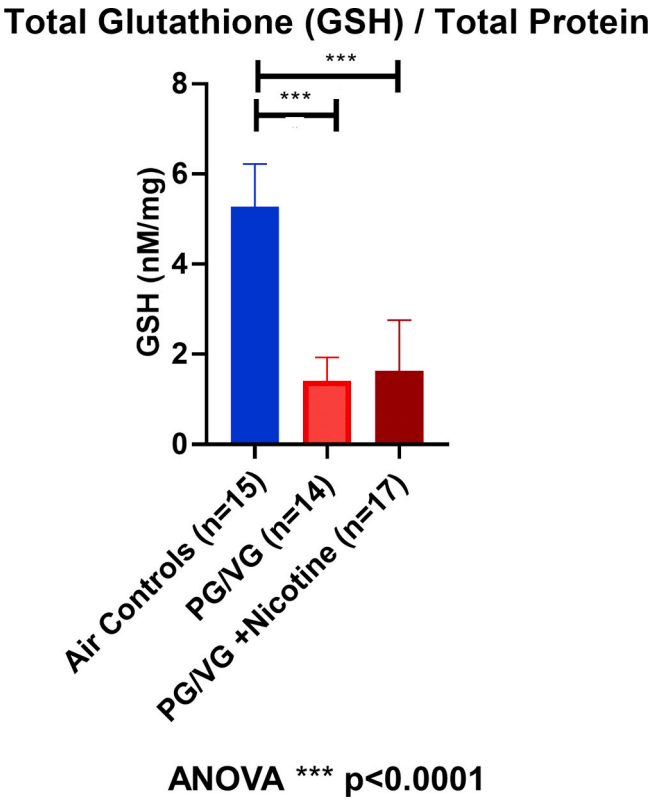

Fig. 2. Total lung glutathione (GSH) assessment. GSH normal for total protein (nM/mg) in air control (5.28 ± 0.95 nM/mg; *blue*; n = 15), PG/VG (1.41 ± 0.52 nM/mg; *red*; n = 14) and PG/VG + (25 mg/ml) Nicotine (1.63 ± 1.12 nM/mg; *dark red*; n = 17) (ANOVA, ****p < 0.0001). (For interpretation of the references to colour in this figure legend, the reader is referred to the Web version of this article.)

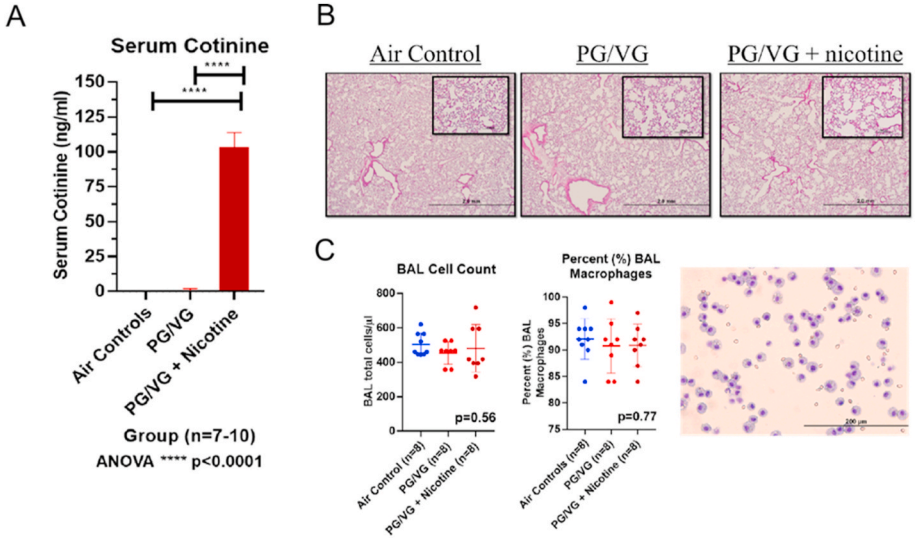

Fig. 1. *In vivo* e-cigarette exposure and biological function. (A) Serum cotinine levels from air controls, PG/VG - propylene glycol/vegetable glycerin, and PG/VG+(25 mg/ml) Nicotine - propylene glycol/vegetable glycerin plus 25 mg/ml nicotine in rats (n = 7–10/group; ANOVA; ****p < 0.0001). (B) Hematoxylin and Eosin (H&E) stained lung sections from animals exposed to air, PG/VG and PG/VG + (25 mg/ml) Nicotine. (C) Bronchoalveolar lavage (BAL) fluid cell count in air controls (503 ± 66 cell/μL), PG/VG (454 ± 65 cell/μL), and PG/VG + (25 mg/ml) Nicotine (481 ± 137 cell/μL) (ANOVA; p = 0.56) and cell differentials with the average macrophage percent in air controls (92 ± 4%), PG/VG (91 ± 5%), and PG/VG + (25 mg/ml) Nicotine (91 ± 4%) (ANOVA; p = 0.77).

3.5. Proteome-wide quantification of thiol oxidation

To quantitatively profile the levels of thiol oxidation at the proteome level in the lung, we employed an established RAC-TMT workflow integrating resin-assisted capture with TMT labeling. Thiopropyl Sepharose 6B resin was used to capture proteins and peptides bearing free thiols from total protein extracts of rats, exposed to either sham air (air control) or PG/VG + 2.5% nicotine (Fig. 3A). In this analysis we only focused on the PG/VG + 2.5% nicotine condition as it represents the more relevant vaping scenario in addition to resource limitation. Endogenous protein free thiols are irreversibly blocked with NEM and reversible thiol oxidations are reduced back to free thiols. The multiplexing capacity of TMT enabled simultaneous analysis of four biological replicates for each of the two treatment conditions. Included in the analysis is a "total thiol" channel, in which the initial NEM blocking step is omitted. This channel represents the combined levels of reduced and oxidized protein thiols, or total thiols present, providing a reference to calculate the site occupancy of thiol oxidation. The peptide signal intensity information obtained by mass spectrometry represents a direct readout of the levels of thiol oxidation or total thiol at a cysteine sites specific level.

Our single-shot MS analysis identified 8705 unique peptides in rat lungs, among which 8506 were cysteine containing peptides bearing free thiols (Supplemental Data 1, Fig. 3B); yielding an enrichment specificity of 97.7% which is in line with the high specificity of resin-assisted capture of protein thiols. The identified peptides covered 6682 unique cysteine sites on 2865 proteins (Fig. 3C). In addition, quantification variation analysis across biological replicates revealed an average Pearson correlation (r) of 0.98 (Figure S1), demonstrating good reproducibility of our workflow in quantifying protein oxidation levels.

Next we sought to evaluate the functional significance of the identified cysteine sites. Cysteine residues play an essential role in protein structure and function as many of them act as the "active site" during catalysis [22]. Significantly, we found 46 unique cysteine sites that are annotated as active sites in Unirpot on 36 proteins, covering key enzymes in a broad range of processes such as thioredoxin (THIO) in antioxidant defense response, ubiquitin-like modifier-activating enzyme 1 (UBA1) in protein degradation, fatty acid synthase (FAS), in cellular energy metabolism, and caspase-3 (CASP3) in apoptosis.

The extensive coverage of the redox proteome in this study prompted us to examine whether oxidation of these cysteine residues has been observed in the literature. Given the lack of deep rat redox proteome reports in the literature, we compared our dataset to that obtained in mouse. Rat and mouse are closely related species with a high degree of similarity between their genomes [23]. A recent study profiled the proteome-wide thiol oxidation in mouse immortalized primary kidney epithelial cells and kidney tissues, providing quantification information on a total of 10,141 unique cysteine sites on 3794 mouse proteins [24]. We thus compared the rat cysteine sites identified here to the available data from the above-mentioned study. Protein homologs from the two species were aligned and the cysteine residue counterparts were further identified. Our data covered 6682 unique rat cysteine sites, among which 1805 sites were also characterized in mouse (Supplemental Data 2).

3.6. E-cig induced alterations of site-specific thiol oxidation

Principal component analysis (PCA) of the redox proteome dataset revealed a partition between e-cig exposed samples and air exposed samples suggesting an e-cig induced alteration of site-specific thiol oxidation (Figure S2). To determine the specific cysteine peptides and sites significantly altered following e-cig exposure, we conservatively applied criteria based on both statistical significance ($p < 0.01$) and a fold change cutoff (at least 20% increase or decrease in the oxidation level). Filtering the 8506 cysteine peptides quantified according to these criteria, our analysis (Fig. 4A) revealed that 300 out of 8506 peptides (3.5%) showed increased oxidation upon exposure to e-cig whereas 64 out of 8506 peptides (0.75%) exhibited a decreased oxidation level of oxidation. The distribution of the total oxidation occupancy also showed an overall shift toward higher oxidation levels under e-cig exposure,

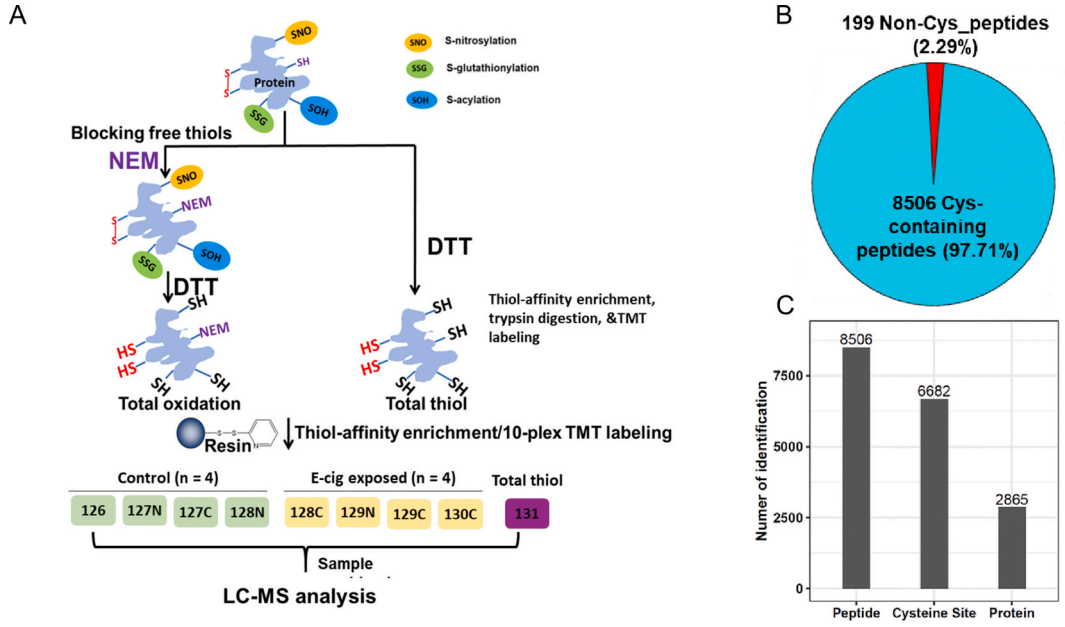

Fig. 3. Redox proteomics analysis of site occupancy of protein thiol total oxidation. (A) The schematic of sample preparation for total oxidation. One arm of tissue samples were processed with NEM blocking for free thiols and followed by DTT for total oxidation. The other arm of samples for total thiol profiling was reduced by DTT without NEM blocking. 4 replicates of control air exposed and 4 replicates of E-cig stimulated rat lung tissues were processed, enriched, and labeled for total oxidation in parallel. A small portion of tissues for each sample were pooled from control and stimulated for total thiol measurements. Thiol-containing peptides were eluted from all 10 labeled samples and combined into one final sample for LC-MS/MS analysis. The total oxidation occupancy was calculated as the ratio of total oxidation over the total thiol for each Cysteine site for a given protein. (B) MS analysis yielded the identified of 8705 unique peptides in rat lungs, among which 8506 were cysteine containing peptides. (C) The identified peptides covered 6682 unique cysteine sites on 2865 proteins.

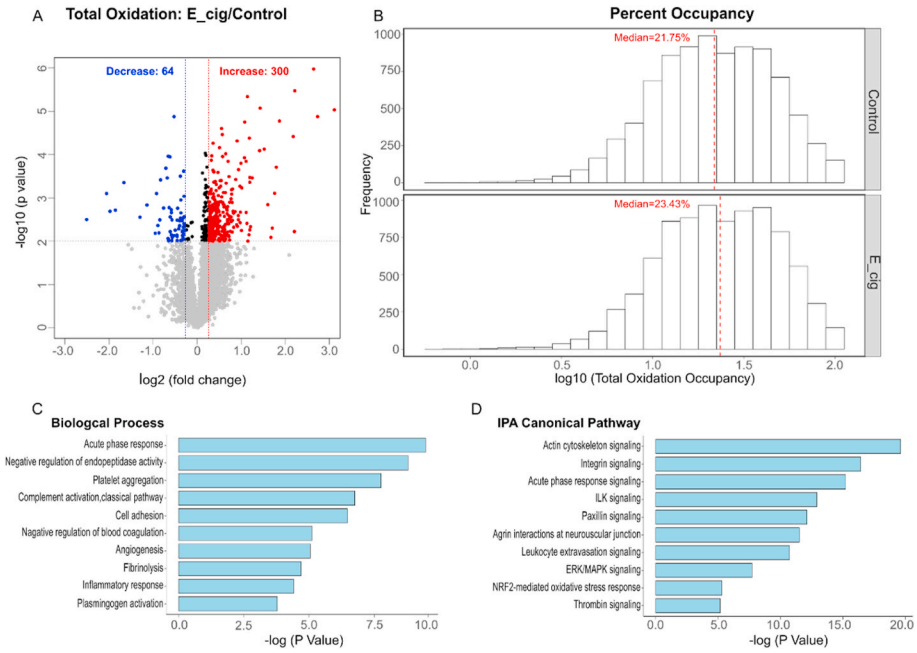

Fig. 4. Oxidative stress-regulated thiol proteome in lung tissue samples. (A) Volcano plot comparing oxidative stress-regulated thiol oxidation levels in samples treated with control to E-cig stimulation. cysteine sites with significantly altered oxidation were indicated in red (increased oxidation) or blue (decreased oxidation), adjusted $p < 0.05$ and FDR = 0.01). (B) On a log scale, a shift in site occupancy is evident between the control (unstimulated) and E-cig (stimulated) samples. (C) DAVID Bioinformatics Resources identified the Biological Processes ranked by significance. (D) Top canonical pathways from IPA analysis. Proteins with significant differences in total oxidation levels were used for the functional analyses. Threshold of significance: $p < 0.05$. (For interpretation of the references to colour in this figure legend, the reader is referred to the Web version of this article.)

with a median occupancy of 21.75% and 23.43% in the control and treated groups, respectively (Fig. 4B). Taken together, the above results suggest that e-cig exposure increases the overall protein oxidation levels and aligns with the notion that cigarette smoke promotes generation of ROS.

We next used the list of 364 peptides (and their corresponding proteins) described above as input for various gene ontology/pathway enrichment tools to examine biological processes and pathways that are modulated by e-cig exposure. Consistent with the notion that e-cigs could exert toxicity in the lung by dysregulation in inflammatory pathways [25], we found significant over-representation of proteins involved in inflammatory response (Fig. 4C). In addition, gene ontology analysis based on both DAVID and Ingenuity Pathway Analysis (IPA) revealed the enrichment of the acute phase response (Fig. 4C and D), suggesting that e-cigs may induce acute-phase response and that these circulating acute-phase proteins may be involved in lung immunity, as reported previously in the case of pneumonia [26].

3.7. Perturbation of ubiquitin-proteasome pathway support redox proteomics observations following E-cig exposure

E-cigarette exposures modified the active sites of multiple ubiquitin-associated proteins (e.g. UBE2N_RAT, B2RYD0_RAT, UFC1_RAT, UBA1_RAT, HERC4_RAT, UBA5_RAT, D3ZNQ6_RAT; Supplemental Data 1). Collectively, these proteins are a group of enzymes used in ubiquitination and protein quality control. Most of the identified proteins are ubiquitin-conjugating enzymes also known as ubiquitin ligases. E1, E2, and E3 ubiquitin-activating enzymes work sequentially to coordinate attachment of ubiquitin with target proteins. Oxidation of certain ubiquitin ligases can impair protein quality control related to ubiquitination including proteasome function, lysosomal processing and endoplasmic reticular stress. Considering a significant portion of ligases identified were related to a ubiquitin proteasome response (UPR), we performed western blots for polyubiquitination, lysine(K)48-linked ubiquitination, and a proteasome 20S functional assay to assess the impact of e-cig oxidation on proteasome-mediated ubiquitination and proteasome function in rat lung tissue. Representative western blots of lung ubiquitin-C (poly-ubiquitination) and lysine(K)48-linked ('proteasome-mediated') ubiquitin expression are depicted in Figure S3. Lung ubiquitin-C (Ubq-C) protein expression normalized for total protein did not increase significantly immediately following the last e-cig exposure (Fig. 5A, $p > 0.9$). K48-linked ubiquitin expression in e-cig-exposed rat lungs also did not increase following e-cig exposure relative to air controls (Fig. 5B, $p > 0.9$). Conversely, proteasome 20S activity increased significantly in e-cig-exposed rat lungs independent of nicotine compared to air controls (Fig. 5C, $^*p < 0.05$). Hence, acute e-cig exposure failed to result in a significant accumulation of polyubiquitinated or K48-linked ubiquitination, however, proteasome 20S activity increased significantly supportive of persistent e-cig oxidative stress inducing proteasome 20S activity.

4. Discussion

In the present study we have used a redox proteomics assay of thiol total oxidation to identify signatures of site-specific protein thiol modifications induced by e-cig exposure to provide new insights into e-cigarette-associated redox signaling in the lung. Our findings support an important role for redox control in the pulmonary response to e-cig exposure and show redox proteomics to be a useful tool for understanding the redox mechanisms associated with e-cig exposure.

4.1. Aerosol characterization, chemical exposure, and nicotine concentrations

The current study used a nose-only inhalation exposure for three 1-h exposure sessions for three consecutive days. Exposures were administered via a nose-only approach to ensure proper reproducibility of aerosol uptake and minimize animal fur deposition. The Sci-Req InExpose aerosol generator was used as a common and commercially available unit for direct comparison with other published literature on electronic nicotine delivery system (ENDS) exposure in rodents [27,28]. The puff profile chosen (75 mL for 3.3 s) is also consistent with those reported by ENDS users where a larger volume is obtained with each puff compared to previous cigarette smoke profiles (average of 55 mL).

In this study, the total particle mass of the generated aerosol (0.968 ± 0.194 mg/mL) was similar to a medium-to-high range e-cigarette exposure as has been characterized previously [8]. The formula adapted from Alexander et al., D = (C x MRV x d/BW), provides a calculated e-liquid dose where D is the dose (mg/kg), C is the concentration in aerosol (mg/L), RMV is the respiratory minute volume (for rats, 0.2

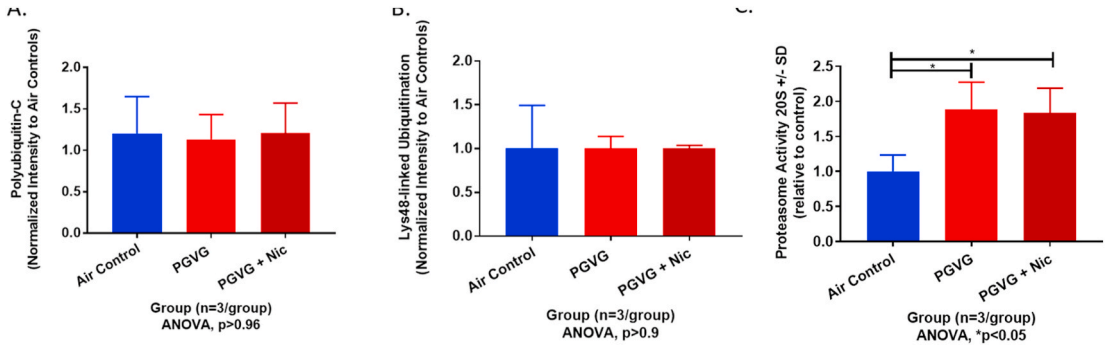

Fig. 5. Ubiquitination expression and proteasome 20S activity in lung tissue samples. Semi-quantification of normalized protein expression by westen blot of (A) ubiquitin-c ('polyubiquitin'), (B) lysine (K)48-linked ('proteasome-mediated') ubiquitin for air control, PG/VG, and PG/VG + (25 mg/ml) Nicotine. (C) Relative proteasome 20S activity among air control, PG/VG and PG/VG + (25 mg/ml) Nicotine (ANOVA, *p < 0.05).

L/min), d is the duration of exposure (180 min), and BW is body weight (kg; for rats, 0.25 kg was used) [29]. Thus, the calculated total e-liquid dose, or human equivalent dose (HED), for these exposures was 139.4 mg/kg. The majority of human users consume less than or equal to 4 mL e-liquid per day [30]. Additionally, most e-liquids vary in proportion of PG and VG, most commonly 50/50 PG/VG [8,12,31]. With these assumptions, the upper limit of normal e-liquid inhalation per day corresponds to 4.6 g total combined mass, or 2.1 g PG in 2 mL of 100% (v/v) PG and 2.5 g VG in 2 mL of 100% (v/v) VG. Hence, the calculated daily dose in a 60 kg adult is 76.7 mg/kg, which is about half the calculated HED for our exposures.

The chosen nicotine concentration was 25 mg/ml (2.5%), which corresponds to approximately 7.2 mg/kg/day per the formula adapted from Alexander et al. [29] Calculating the HED based on body surface area by dividing the rat dose by a factor of 6.2 yields a HED of 1.2 mg/kg, or 72 mg for a 60 kg adult [32]. Assuming a human inhales around 4 mL e-liquid per day and the maximum nicotine concentration in e-liquid under the European Tobacco Products Directive (TPD Article 20, 3. B) recommends 20 mg/mL, average nicotine inhalation per day is 80 mg for a 60 kg adult. Hence, the calculated HED is below the presumed human inhalation average, however, human inhalation of nicotine is changing rapidly. Additionally, outside of Europe, nicotine concentration is currently not restricted to 20 mg/mL where certain e-liquid now contains upwards of 5% by volume, equivalent to 59 mg/ml [33], hence, nicotine in some cartridges greatly exceed the concentration targeted in our exposures.

In line with the above listed nicotine concentrations, the mean plasma cotinine levels are similar to those published by McGrath-Morrow et al. [21] In neonatal mice exposed to 1.8% nicotine/PG the mean plasma cotinine level was 62.3 ± 3.3 ng/mL [21]. The mean plasma cotinine in the current study of rats exposed to 2.5% nicotine/50PG/50VG was 103.3 ± 10.5 ng/mL. Conversely, this means cotinine level is significantly lower than reported by Werley et al. (413 ± 59 ng/ml) [31], where Sprague-Dawley rats were exposed to 2.0% nicotine PG/VG mixture for 160 min for 28 days. Multiple factors likely affect cotinine levels including timing with respect to euthanasia (immediately after last exposure), direct nose-only exposure (versus secondary or tertiary exposure), nicotine metabolism, and the higher concentration of total e-liquid (discussed above). Collectively, our exposures model a high exposure for a short period similar to the puff profiles of ENDS users seeking high nicotine concentrations for shorter exposure periods.

4.2. Histopathology

To better characterize the lung response to acute e-cig exposure, we performed histologic fixation and staining of left lungs on all exposed animals. As demonstrated in Fig. 1B, macroscopic evaluation of PG/VG-exposed rat lungs did not differ significantly from air control rat lungs. More specifically, lung architecture was preserved without notable changes in parenchymal or airway structure. Additionally, the lung parenchyma did not appear with increased inflammation in PG/VG-exposed to air controls. There was mild heterogeneity in lung expansion of PG/VG and PG/VG + nicotine exposed lungs of the lung parenchyma with areas of hyper-expansion and adjacent atelectasis. These changes can be seen with central airway obstruction from mucus hyperplasia [12], similar to acute (3-day) exposure in mice [12,34]. Preserved lung structure has also held true for rodents exposed to e-cigarette aerosols containing PG/VG or PG/VG plus nicotine chronically [8,9,31]. In contrast, neonatal mice exposed to e-cigarette aerosol for 10 days immediately after birth demonstrated significantly reduced alveolarization by mean linear intercept [21]. Hence, rodents exposed to e-cigarette during lung development may be at greater risk for impaired lung alveolarization over adolescent or adult rodents exposed to e-cigarette aerosols, considering no appreciable change in lung histology was present following our acute e-cigarette exposure.

4.3. BALF total cell number and cell count

Similar to the changes observed with histology, PG/VG nor PG/VG + nicotine aerosol exposure failed to induce a significant change in total cell number or percentage of macrophage present in BALF. Prior published literature is extremely heterogeneous with regards to acute changes in BALF total cell count and macrophage percentage for e-cigarette exposure. Most likely, these differences are due to differences in e-liquid composition, exposure duration, animal strain and timing of euthanasia after exposure cessation. Glynos et al. showed increased BALF total cell count and macrophage number after 3 days of PG/VG exposure [12], while Lerner et al. demonstrated no change in total BALF number nor number of macrophages [11]. Both exposures lasted for 3 days, but different coil composition (nickel versus chromium) may have contributed to differences in BALF cell number and percentage of macrophages. In line with our acute BALF results, chronic e-cigarette exposure in rodents to PG/VG or PG/VG + nicotine also does not appear to change the total number of BALF cells or BALF macrophages [6,9,12,31].

4.4. Surrogate marker of oxidative stress: reduced total lung glutathione

Our primary hypothesis for this study was acute e-cigarette exposure would significantly reduce the lung's oxidative capacity. Indeed, after only a 3-day e-cigarette aerosol exposure, a significant reduction of normalized total lung glutathione occurred. Surprisingly, this reduction in total lung glutathione was most significant when comparing air controls to PG/VG alone. The addition of nicotine to PG/VG did not promote any additional reduction in total lung glutathione. This response is likely time-dependent as has been seen acutely after cigarette smoke exposure in rodents. When mice are euthanized immediately

after cigarette exposure, the lung's total amount of glutathione is reduced similar to e-cigarette exposure [35,36]. With regards to e-cigarette exposure, prior authors have also shown that acute e-cigarette exposure in mice reduces intracellular glutathione levels in lungs after 3 days of exposure [11]. Unique to this work, we have done additional redox proteomics on exposed lungs for providing a more comprehensive evaluation of oxidation following e-cigarette exposure.

4.5. *Proteome-wide assessment of oxidative stress following exposure to e-cig*

The impact of e-cig exposure on the redox homeostasis of rat lung was evaluated by measuring proteome-wide thiol oxidation, which revealed several key findings. First, we found that e-cig (PG/VG + nicotine) exposure leads to a systematic increase in protein thiol oxidation (Fig. 4A), reflecting an overall more oxidized redox status. Together with the decreased level of GSH, this suggests that PG/VG + nicotine exposure-derived ROS could overwhelm the antioxidant defense system, resulting in oxidative stress in the lung with an increase in protein oxidation. The profound perturbation of the redox proteome is striking, given that PG/VG + nicotine administration in this study did not cause a significant change in BAL cell count or BAL macrophage (Fig. 1C). This supports the notion that the thiol redox proteome is more sensitive sentinel of cellular health and may precede any phenotypical changes. Second, our large-scale profiling of the lung redox proteome revealed that cysteine residues assume a wide range of oxidation occupancy with different sensitivity in response to PG/VG + nicotine exposure (Supplemental Data 1). Interestingly, some of the most significantly changed sites are on proteins that are key members of the protein quality control process, for example PDIA5 and PSME2. A number of prior reports have suggested exposure to traditional cigarette smoke alters the three-dimensional structure of PDI, inhibiting PDI reductase and isomerase activity [37–39]. How the increased oxidation on PDIA5, and PSME2, affect their activity/function and role in the protein quality control process following exposure to e-cig aerosol is at present unclear and beyond the scope of this study. However, our data provides important clues to direct further detailed investigations.

Pathway enrichment analysis identified endothelial biology, coagulation, and complement activation being upregulated in rat lung homogenates after acute short-term e-cigarette aerosol exposure. Common proteins upregulated in multiple pathways included Complement C3 (C3), Kininogen 1 (KNG1), Complement C5 (C5), T-kininogen 1 (KNT1), Fibrinogen alpha chain and Complement component 4A (C4A). Combustible smoke exposure is a well-known cardiovascular risk factor, independent of other traditional risk factors such as hypertension, dyslipidemia, or diabetes [40]. Hence, combustible tobacco products impart cardiovascular injury through mechanisms distinct from traditional CVD risk factors. One of the primary mechanisms identified is through increased thrombosis. Smoking is strongly associated with increased circulating markers of thrombogenesis, including D-dimer, fibrinogen, and homocysteine [41]. Chronic smoke exposure also increases thrombopoietin, a known trigger of platelet activation and subsequent thrombosis through platelet-monocyte adhesion [41]. Investigation of the effects of non-combustible products, such as e-cigarettes, on platelet activation and thrombosis remains in its infancy. Hom et al. exposed platelets isolated from healthy volunteer whole blood to tobacco smoke extracts, e-cig aerosol extracts, and pure nicotine [42]. Exposure of platelets to e-cig aerosol extracts induced a significant upregulation of pro-inflammatory gC1qR and cC1qR expression with increased deposition of C3b. Platelet activation, aggregation, and adhesion potential were also enhanced after e-cig extract exposure. These changes were independent of nicotine concentration. Conversely, platelet exposure to pure nicotine inhibited platelet function. Barber et al. extended this work to the effects of e-cigarette extract exposure on endothelial cells [43]. Endothelial cells were exposed to e-cig or cigarette extracts, and then assessed for inflammation, viability, and complement expression. A significant increase in complement deposition and C1q receptor expression occurred after e-cigarette extract exposure. These results were again independent of nicotine concentration. Nocella et al. identified similar effects in adult smokers and non-smokers [44]. Within 5 min of inhaling e-cigarette aerosol, increased levels of sP-selectin, sCD40L and platelet aggregation occurred in both smokers and non-smokers, implicating short-term effects of e-cigarette exposure on platelet activation. Hence, similar to combustible cigarette exposure, short-term exposure to e-cigarette aerosols promotes complement and platelet activation independent of nicotine concentration.

4.6. *Perturbations in the ubiquitin proteasome pathway*

Pathway enrichment also identified a significant number of modifications to ubiquitin-associated proteins following e-cigarette exposure. Proteolysis is critical to maintaining cellular homeostasis, especially with respect to timely degradation of oxidized proteins. We semi-quantitated total rat lung polyubiquitination and proteasome-mediated polyubiquitination using ubiquitin-C and lysine(K)-48-linked ubiquitination, respectively. Surprisingly, the total amount of polyubiquitinated proteins were not significantly increased in e-cig-exposed rat lungs with and without nicotine compared to air controls. However, proteasome 20S activity increased significantly in both PG/VG and PG/VG + N exposed rat lungs compared to air controls. Two possible explanation for the lack of accumulation of polyubiquitinated proteins include: (1) the compensatory increase in proteasome 20S activity promoted proper protein degradation prior to polyubiquitinated protein accumulation, or (2) the timing of euthanasia (immediately after exposure) occurred before polyubiquitination occurred. We hypothesize the former is more likely than the latter considering e-cigarette exposures were short-term (3 days of 3 h per day), which is likely insufficient to functionally impair the proteolytic system and allow for oxidized proteins to aggregate [45]. Future evaluation and targeting of the ubiquitin proteasome pathway may be valuable in preventing the pathologic consequences of chronic e-cigarette exposure.

5. Conclusions

The present study demonstrates that acute e-cig exposure induces oxidative stress in the lungs without discernable changes in lung structure or pulmonary inflammatory response. A redox proteomics assay elucidated the site-specific changes in protein thiol oxidation induced by acute e-cig exposure. Statistical analysis revealed the oxidation levels of 350 cysteine-containing peptides were significantly altered by e-cig exposure, inducing perturbations of protein quality control, cell adhesion, immune system and redox homeostasis. Our study highlights the important role of redox control in the pulmonary response to e-cig exposure and also demonstrates the utility of redox proteomics as a tool for elucidating the molecular mechanisms underlying this response.

Declaration of competing interest

The authors declare that they have no known competing financial interests or personal relationships that could have appeared to influence the work reported in this paper.

Acknowledgements

This work was supported by the National Institutes of Health/National Heart Lung Blood Institute grant number R01 HL139335 and by the National Institute of Environmental Health Sciences (P30 ES001247). Parts of this research was performed in the Environmental Molecular Sciences Laboratory (EMSL), a national scientific user facility sponsored by the Department of Energy (DOE) and located at PNNL, which is operated by Battelle Memorial Institute for the DOE under

Contract DE-AC05-76RL0 1830.

Appendix A. Supplementary data

Supplementary data to this article can be found online at https://doi.org/10.1016/j.redox.2020.101758.

References

[1] R. Polosa, Electronic cigarette use and harm reversal: emerging evidence in the lung, BMC Med. 13 (2015) 54, https://doi.org/10.1186/s12916-015-0298-3.

[2] K.O. Fagerström, K. Bridgman, Tobacco harm reduction: the need for new products that can compete with cigarettes, Addict, Beyond Behav. 39 (2014) 507–511, https://doi.org/10.1016/j.addbeh.2013.11.002.

[3] P. Callahan-Lyon, Electronic cigarettes: human health effects, Tobac. Contr. 23 (2014) ii36–40, https://doi.org/10.1136/tobaccocontrol-2013-051470.

[4] P.S. Hiemstra, R. Bals, Basic science of electronic cigarettes: assessment in cell culture and in vivo models, Respir. Res. 17 (2016), https://doi.org/10.1186/s12931-016-0447-z.

[5] M.S. Werley, P. McDonald, P. Lilly, D. Kirkpatrick, J. Wallery, P. Byron, J. Venitz, Non-clinical safety and pharmacokinetic evaluations of propylene glycol aerosol in Sprague-Dawley rats and Beagle dogs, Toxicology 287 (2011) 76–90, https://doi.org/10.1016/j.tox.2011.05.015.

[6] B. Phillips, M. Esposito, J. Verbeeck, S. Boué, A. Iskandar, G. Vuillaume, P. Leroy, S. Krishnan, U. Kogel, A. Utan, W.K. Schlage, M. Bera, E. Veljkovic, J. Hoeng, M. C. Peitsch, P. Vanscheeuwijck, Toxicity of aerosols of nicotine and pyruvic acid (separate and combined) in Sprague-Dawley rats in a 28-day OECD 412 inhalation study and assessment of systems toxicology, Inhal. Toxicol. 27 (2015) 405–431, https://doi.org/10.3109/08958378.2015.1046000.

[7] A. Lechasseur, E. Jubinville, J. Routhier, J.C. Bérubé, M. Hamel-Auger, M. Talbot, J. Lamothe, S. Aubin, M.È. Paré, M.J. Beaulieu, Y. Bossé, C. Duchaine, M. C. Morissette, Exposure to electronic cigarette vapors affects pulmonary and systemic expression of circadian molecular clock genes, Physiol. Rep. 5 (2017), https://doi.org/10.14814/phy2.13440.

[8] B. Phillips, B. Titz, U. Kogel, D. Sharma, P. Leroy, Y. Xiang, G. Vuillaume, S. Lebrun, D. Sciuscio, J. Ho, C. Nury, E. Guedj, A. Elamin, M. Esposito, S. Krishnan, W.K. Schlage, E. Veljkovic, N.V. Ivanov, F. Martin, M.C. Peitsch, J. Hoeng, P. Vanscheeuwijck, Toxicity of the main electronic cigarette components, propylene glycol, glycerin, and nicotine, in Sprague-Dawley rats in a 90-day OECD inhalation study complemented by molecular endpoints, Food Chem. Toxicol. 109 (2017) 315–332, https://doi.org/10.1016/j.fct.2017.09.001.

[9] M.C. Madison, C.T. Landers, B.H. Gu, C.Y. Chang, H.Y. Tung, R. You, M.J. Hong, N. Baghaei, L.Z. Song, P. Porter, N. Putluri, R. Salas, B.E. Gilbert, I. Levental, M. J. Campen, D.B. Corry, F. Kheradmand, Electronic cigarettes disrupt lung lipid homeostasis and innate immunity independent of nicotine, J. Clin. Investig. 129 (2019) 4290–4304, https://doi.org/10.1172/JCI128531.

[10] S. Cirillo, F. Vivarelli, E. Turrini, C. Fimognari, S. Burattini, E. Falcieri, M.B. L. Falcieri, V. Cardenia, M.T. Rodriguez-Estrada, M. Paolini, D. Canistro, The customizable e-cigarette resistance influences toxicological outcomes: lung degeneration, inflammation, and oxidative stress-induced in a rat model, Toxicol. Sci. 172 (2019) 132–145, https://doi.org/10.1093/toxsci/kfz176.

[11] C.A. Lerner, I.K. Sundar, H. Yao, J. Gerloff, D.J. Ossip, S. McIntosh, R. Robinson, I. Rahman, Vapors produced by electronic cigarettes and e-juices with flavorings induce toxicity, oxidative stress, and inflammatory response in lung epithelial cells and in mouse lung, PLoS One 10 (2015), https://doi.org/10.1371/journal.pone.0116732.

[12] C. Glynos, S.I. Bibli, P. Katsaounou, A. Pavlidou, C. Magkou, V. Karavana, S. Topouzis, I. Kalomenidis, S. Zakynthinos, A. Papapetropoulos, Comparison of the effects of e-cigarette vapor with cigarette smoke on lung function and inflammation in mice, Am. J. Physiol. Lung Cell Mol. Physiol. 315 (2018) 662–672, https://doi.org/10.1152/ajplung.00389.2017.

[13] J. Duan, V.K. Kodali, M.J. Gaffrey, J. Guo, R.K. Chu, D.G. Camp, R.D. Smith, B. D. Thrall, W.J. Qian, Quantitative profiling of protein s-glutathionylation reveals redox-dependent regulation of macrophage function during nanoparticle-induced oxidative stress, ACS Nano 10 (2016) 524–538, https://doi.org/10.1021/acsnano.5b05524.

[14] D. Su, M.J. Gaffrey, J. Guo, K.E. Hatchell, R.K. Chu, T.R. Clauss, J.T. Aldrich, S. Wu, S. Purvine, D.G. Camp, R.D. Smith, B.D. Thrall, W.J. Qian, Proteomic identification and quantification of S-glutathionylation in mouse macrophages using resin-assisted enrichment and isobaric labeling, Free Radic. Biol. Med. 67 (2014) 460–470, https://doi.org/10.1016/j.freeradbiomed.2013.12.004.

[15] J. Guo, M.J. Gaffrey, D. Su, T. Liu, D.G. Camp, R.D. Smith, W.J. Qian, Resin-assisted enrichment of thiols as a general strategy for proteomic profiling of cysteine-based reversible modifications, Nat. Protoc. 9 (2014) 64–75, https://doi.org/10.1038/nprot.2013.161.

[16] P.A. Kramer, J. Duan, M.J. Gaffrey, A.K. Shukla, L. Wang, T.K. Bammler, W.J. Qian, D.J. Marcinek, Fatiguing contractions increase protein S-glutathionylation occupancy in mouse skeletal muscle, Redox. Biol. 17 (2018) 367–376, https://doi.org/10.1016/j.redox.2018.05.011.

[17] J. Duan, T. Zhang, M.J. Gaffrey, K.K. Weitz, R.J. Moore, X.L. Li, M. Xian, B. D. Thrall, W.J. Qian, Stochiometric quantification of the thiol redox proteome of macrophages reveals subcellular compartmentalization and susceptibility to oxidative perturbations, Redox. Biol. 36 (2020), https://doi.org/10.1016/j.redox.2020.101649.

[18] S. Kim, P.A. Pevzner, MS-GF plus makes progress towards a universal database search tool for proteomics, Nat. Commun. 5 (2014), https://doi.org/10.1038/ncomms6277.

[19] M.E. Monroe, J.L. Shaw, D.S. Daly, J.N. Adkins, R.D. Smith, MASIC: a software program for fast quantitation and flexible visualization of chromatographic profiles from detected LC-MS(/MS) features, Comput. Biol. Chem. 32 (2008) 215–217, https://doi.org/10.1016/j.compbiolchem.2008.02.006.

[20] Y.A. Chiao, H. Zhang, M. Sweetwyne, J. Whitson, S. Ting, N. Basisty, L. Pino, E. Quarles, N. Nguyen, M.D. Campbell, T. Zhang, M.J. Gaffrey, G. Merrihew, L. Wang, Y. Yue, D. Duan, H. Granzier, H.H. Szeto, W.J. Qian, Late-life restoration of mitochondrial function reverses cardiac dysfunction in old mice, bioRxiv (2020), https://doi.org/10.1101/2020.01.02.893008.

[21] S.A. McGrath-Morrow, M. Hayashi, A. Aherrera, A. Lopez, A. Malinina, J. M. Collaco, E. Neptune, J.D. Klein, J.P. Winickoff, P. Breysse, P. Lazarus, G. Chen, The effects of electronic cigarette emissions on systemic cotinine levels, weight and postnatal lung growth in neonatal mice, PLoS One 10 (2015), https://doi.org/10.1371/journal.pone.0118344.

[22] C. Klomsiri, P.A. Karplus, L.B. Poole, Cysteine-based redox switches in enzymes, Antioxid. Redox Signal. 14 (2011), https://doi.org/10.1089/ars.2010.3376.

[23] S. Zhao, J. Shetty, L. Hou, A. Delcher, B. Zhu, K. Osoegawa, P. de Jong, W. C. Nierman, R.L. Strausberg, C.M. Fraser, Human, mouse, and rat genome large-scale rearrangements: stability versus speciation, Genome Res. 14 (2004) 1851–1860, https://doi.org/10.1101/gr.2663304.

[24] J. van der Reest, S. Lilla, L. Zheng, S. Zanivan, E. Gottlieb, Proteome-wide analysis of cysteine oxidation reveals metabolic sensitivity to redox stress, Nat. Commun. 9 (2018) 1581, https://doi.org/10.1038/s41467-018-04003-3.

[25] P.G. Shields, M. Berman, T.M. Brasky, J.L. Freudenheim, E. Mathe, J.P. McElroy, M.A. Song, M.D. Wewers, A review of pulmonary toxicity of electronic cigarettes in the context of smoking: a focus on inflammation, Cancer Epidemiol. Biomark. Prev. 26 (2017) 1175–1191, https://doi.org/10.1158/1055-9965.EPI-17-0358.

[26] K.L. Hilliard, E. Allen, K.E. Traber, K. Yamamoto, N.M. Stauffer, G.A. Wasserman, M.R. Jones, J.P. Mizgerd, L.J. Quinton, The lung-liver axis: a requirement for maximal innate immunity and hepatoprotection during pneumonia, Am. J. Respir. Cell Mol. Biol. 53 (2015) 378–390, https://doi.org/10.1165/rcmb.2014-0195OC.

[27] H.L. Shi, X.M. Fan, A. Horton A, S.T. Haller, D.J. Kennedy, I.T. Schiefer, L. D. Dworkin, C.J. Cooper, J. Tian, The effect of electronic-cigarette vaping on cardiac function and angiogenesis in mice, Sci. Rep. 9 (2019), https://doi.org/10.1038/s41598-019-40847-5.

[28] J.H. Hwang, M. Lyes, K. Sladewski, .E. McEachern, D.P. Mathew, S. Das, A. Moshensky, S. Bapat, D.T. Pride, W.M. Ongkeko, L.E. Crotty Alexander, Electronic cigarette inhalation alters innate immunity and airway cytokines while increasing the virulence of colonizing bacteria, J. Mol. Med. 94 (2016) 667–679, https://doi.org/10.1007/s00109-016-1378-3.

[29] D.J. Alexander, C.J. Collins, D.W. Coombs, I.S. Gilkison, C.J. Hardy, G. Healey, G. Karantabias, N. Johnson, A. Karlsson, J.D. Kilgour, P. McDonald, Association of inhalation toxicologists (AIT) working party recommendation for standard delivered dose calculation and expression in non-clinical aerosol inhalation toxicology studies with pharmaceuticals, Inhal. Toxicol. 20 (2008) 1179–1189, https://doi.org/10.1080/08958370802207318.

[30] Action on Smoking and Health, Use of electronic cigarettes (vapourisers) among adults in great britain. Ash. Action on smoking and health. https://ash.org.uk/wp-content/uploads/2019/06/ASH-Factsheet-Youth-E-cigarette-Use-2019.pdf, 2019.

[31] M.S. Werley, D.J. Kirkpatrick, M.J. Oldham, A.M. Jerome, T.B. Langston, P.D. Lilly, D.C. Smith, W.J. Mckinney Jr., Toxicological assessment of a prototype e-cigaret device and three flavor formulations: a 90-day inhalation study in rats, Inhal. Toxicol. 28 (2016) 22–38, https://doi.org/10.3109/08958378.2015.1130758.

[32] CDER (Center for Drug Evaluation and Research), Guidance for industry estimating the maximum safe starting dose in initial clinical trials for therapeutics in adult healthy volunteers, Accessed from, https://www.fda.gov/media/72309/download, 2005.

[33] E.E. Omaiye, K.J. McWhirter, W.T. Luo, J.F. Pankow, P. Talbot, High-nicotine electronic cigarette products: toxicity of JUUL fluids and aerosols correlates strongly with nicotine and some flavor chemical concentrations, Chem. Res. Toxicol. 32 (2019) 1058–1069, https://doi.org/10.1021/acs.chemrestox.8b00381.

[34] A. Husari, A. Shihadeh, S. Talih, Y. Hashem, M. El Sabban, G. Zaatari, Acute exposure to electronic and combustible cigarette aerosols: effects in an animal model and in human alveolar cells, Nicotine Tob. Res. 18 (2016) 613–619, https://doi.org/10.1093/ntr/ntv169.

[35] N.S. Gould, E. Min, J. Huang, H.W. Chu, J. Good, R.J. Martin, B.J. Day, Glutathione depletion accelerates cigarette smoke-induced inflammation and airspace enlargement, Toxicol. Sci. 147 (2015) 466–474, https://doi.org/10.1093/toxsci/kfv143.

[36] N.S. Gould, B.J. Day, Targeting maladaptive glutathione responses in lung disease, Biochem. Pharmacol. 81 (2011) 187–193, https://doi.org/10.1016/j.bcp.2010.10.001.

[37] H. Kenche, Z.W. Ye, K. Vedagiri, D.M. Richards, X.H. Gao, K.D. Tew, D. M. Townsend, A. Blumental-Perry, Adverse outcomes associated with cigarette smoke radicals related to damage to protein-disulfide isomerase, J. Biol. Chem. 291 (2016) 4763–4778, https://doi.org/10.1074/jbc.M115.712331.

[38] H. Kenche, C.J. Baty, K. Vedagiri, S.D. Shapiro, A. Blumental-Perry, Cigarette smoking affects oxidative protein folding in endoplasmic reticulum by modifying protein disulfide isomerase, Faseb. J. 27 (2013) 965–977, https://doi.org/10.1096/fj.12-216234.

[39] S.G. Kelsen, X.B. Duan, R. Ji, O. Perez, C. Liu, S. Merali, Cigarette smoke induces an unfolded protein response in the human lung - a proteomic approach, Am. J. Respir. Cell Mol. Biol. 38 (2008) 541–550, https://doi.org/10.1165/rcmb.2007-0221OC.

[40] D.J. Conklin, S. Schick, M.J. Blaha, A. Carll, A. DeFilippis, P. Ganz, M.E. Hall, N. Hamburg, T. O'Toole, L. Reynolds, S. Srivastava, A. Bhatnagar, Cardiovascular injury induced by tobacco products: assessment of risk factors and biomarkers of harm. A tobacco centers of regulatory science compilation, Am. J. Physiol. Heart Circ. Physiol. 316 (2019) 801–827, https://doi.org/10.1152/ajpheart.00591.2018.

[41] E. Lupia, A. Goffi, O. Bosco, G. Montrucchio, Thrombopoietin as biomarker and mediator of cardiovascular damage in critical diseases, Mediat. Inflamm. (2012), https://doi.org/10.1155/2012/390892.

[42] S. Hom, L. Chen, T. Wang, B. Ghebrehiwet, W. Yin, D.A. Rubenstein, Platelet activation, adhesion, inflammation, and aggregation potential are altered in the presence of electronic cigarette extracts of variable nicotine concentrations, Platelets 27 (2016) 694–702, https://doi.org/10.3109/09537104.2016.1158403.

[43] K.E. Barber, B. Ghebrehiwet, W. Yin, D.A. Rubenstein, Endothelial cell inflammatory reactions are altered in the presence of e-cigarette extracts of variable nicotine, Cel, Mol. Bioeng. 10 (2017) 124–133, https://doi.org/10.1007/s12195-016-0465-4.

[44] C. Nocella, G. Biondi-Zoccai, S. Sciarretta, M. Peruzzi, F. Pagano, L. Loffre, P. Pignatelli, C. Bullen, G. Frati, Impact of tobacco versus electronic cigarette smoking on platelet function, Am. J. Cardiol. 122 (2018) 1477–1481, https://doi.org/10.1016/j.amjcard.2018.07.029.

[45] M. Pajares, N. Jiménez-Moreno, I.H.K. Dias, B. Debelec, M. Vucetic, K.E. Fladmark, H. Basaga, S. Ribaric, I. Milisav, A. Cuadrado, Redox control of protein degradation, Redox. Biol. 6 (2015) 409–420, https://doi.org/10.1016/j.redox.2015.07.003.